COMPUTER TECHNOLOGIES
IN PHYSICS

Vector Finder—A Toolkit for Track Finding in the MPD Experiment

Dmitrii Zinchenko[a, *], Alexander Zinchenko[a], and Eduard Nikonov[b]

[a]VBLHEP, Joint Institute for Nuclear Research, Dubna, Moscow oblast, 141980 Russia
[b]LIT, Joint Institute for Nuclear Research, Dubna, Moscow oblast, 141980 Russia
***e-mail: zinchenk1994@gmail.com**

Abstract—A track reconstruction method based on a constrained combinatorial search for track candidates, i.e. combinations of detector hits possibly belonging to a track, is presented. The algorithm has been implemented as a Vector Finder software toolkit containing a track reconstruction procedure and tools to determine hit acceptance windows (a priori constraints) for the track search. Track reconstruction results for high multiplicity simulated events ($\sim$1000 particles in the detector acceptance) are shown demonstrating good performance of the approach proposed.

1. INTRODUCTION

With a completion of the civil construction stage of the NICA complex [1] and beginning of the MPD detector assembly work, the MPD experiment [2] moves into the following stage of its preparation for data taking. Although the detector commissioning and experiment start-up are still ahead, some activity on evaluating the project's future has already started.

As one of the possible MPD upgrade steps, an Inner Tracking System (ITS) based on the next generation silicon pixel detectors MAPS [3] is being considered to be installed between the beam pipe and the Time Projection Chamber (TPC) (Fig. 1). It is expected that such a detector will increase the research potential of the experiment for both the proton-proton (high luminosity) and nucleus-nucleus (high particle multiplicity) interactions. According to the proposed design, the MPD ITS will consist of five layers of silicon pixel detectors. The main purpose of the ITS is to improve quality and provide better precision of track, primary and secondary vertex reconstruction in MPD in the region close to the interaction point. These goals will be achieved due to higher acceptance of the ITS in pseudorapidity η and transverse momentum p_T of tracks because of its closer proximity to the beam line (~3 cm instead of ~40 cm in the TPC) and excellent spatial resolution (<10 μm in each direction as compared with ~0.5 and ~1 mm in transverse and longitudinal directions, respectively, for the TPC).

In order to study the upgraded detector performance the track reconstruction method based on the Kalman filtering approach, developed for the MPD TPC, was modified to add ITS hits to extrapolated tracks according to the Kalman filter formalism. However, given the significant difference in hit position precision in TPC and ITS one can expect that such a TPC-based tracking might not be the optimal one. Moreover, the ITS stand-alone track reconstruction can be useful for detector alignment purposes as well as for development of a high-level trigger in ITS for future high luminosity running in *pp*-mode. Therefore, another approach to ITS track reconstruction was developed [4, 5], which eventually evolved in a more general paradigm implemented as a so-called Vector Finder toolkit, containing software instruments for a realisation of a self-contained system for track reconstruction in high energy physics experiments. This toolkit is described below along with its application results to track reconstruction in the MPD ITS.

2. METHOD DESCRIPTION

The track finding method is based on the combinatorial search for detector hit combinations which can potentially belong to the same particle. Here a hit is a reconstructed point of a particle trajectory crossing of a detector layer. The procedure starts from creating vectors connecting hits on either two inner or two outer detector layers (depending on the algorithm modification) with overall outward or inward directions, respectively. The range of the directions, i.e. acceptable hit pair combinations, should be compatible with event topology as will be explained in the following. Further explanations and application details are given for the algorithm modification with the inward track following direction which has an advantage of starting from the region with lower hit density. So, the algorithm goes inward and adds hits (builds
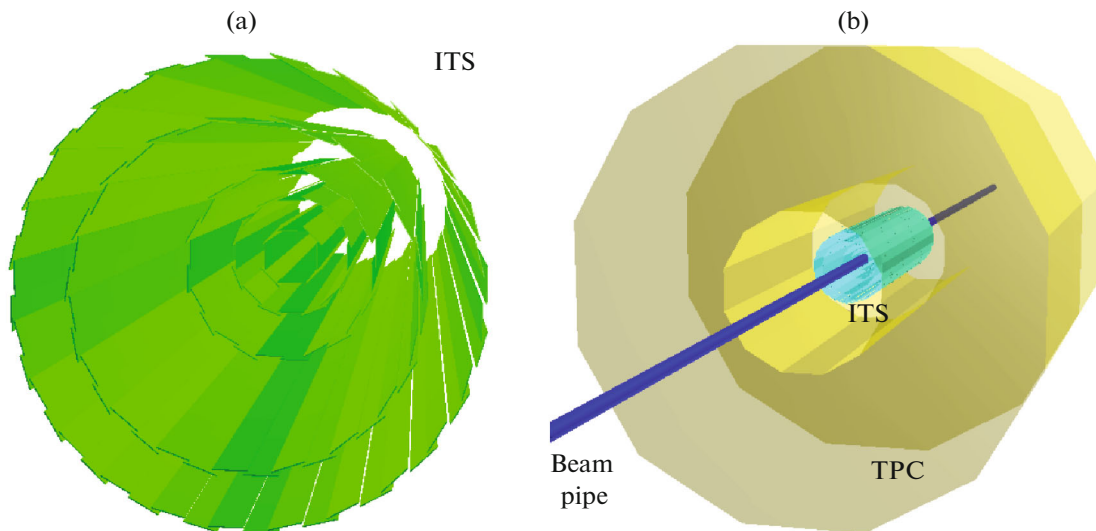
Fig. 1. (a) 5-layer ITS geometry. (b) ITS+TPC model. Overall dimensions of the ITS and TPC are $r_{min} \sim 3$ cm, $r_{max} \sim 20$ cm, half-length ~ 75 cm and $r_{min} \sim 40$ cm, $r_{max} \sim 120$ cm, half-length ~ 170 cm, respectively.

continuation vectors) on the sequential layers within some windows defined by a priori constraints coming from the detector geometry and event characteristics (momentum and angular spectra of particles to be reconstructed). These windows reduce combinatorics and bring the processing time to practical values. The processing time can also be decreased by designing the tracking procedure in such a way to perform the hit selection either by using precomputed values for a given event (if possible) or using values obtained at the previous selection step (previous layers). The collected hit combinations (track candidates) are fitted by the Kalman filter to verify hit-to-track associations and yield track parameters.

From the just mentioned considerations concerning the hit selection approach, two different cases should be distinguished, namely, primary and secondary tracks.

2.1. Primary Tracks

Primary tracks are produced in the primary vertex, i.e. the collision point of two beams in colliders or the interaction point of the incoming beam and the target in fixed target experiments. In fixed target experiments the interaction point is usually well localized, while in collider experiments the longitudinal position can vary in quite a large interval. However, in heavy ion collisions with high multiplicity of produced primary particles the vertex position can be determined in each event with rather high precision before track reconstruction using a well-known vertex position estimator based on combinations of hit pairs. Therefore, the acceptance window determination procedure can use precomputed values such as hit azimuthal and polar angles in the coordinate system with Z-axis directed along the beam line, Y-axis vertically upward and X-axis horizontally. The polar angle *theta* is the angle between the beam line (Z-axis) and the vector from the interaction point to the hit (Fig. 2). The azimuthal angle is the angle between the X-axis and the vector from the interaction point to the hit projection on the transverse XY-plane. Hits can be ordered according to their corresponding angles.

In the longitudinal projection the magnetic field directed along Z does not affect the track trajectory, so tracks can be considered as straight lines (see the schematic picture in Fig. 2a). Therefore, track candidates can attach hits from the next detector layer with sufficiently close polar angles, i.e. the track candidate containing the last accepted hit with the polar angle *theta* can be extended with the hits from the next layer in the window $\pm epsth$ (Fig. 2a) provided their azimuthal angles are also consistent.

In the transverse projection charged particle trajectories are close to circle arcs because of the magnetic field influence. Therefore, only hits corresponding to the current track candidate curvature (i.e. particle transverse momentum) should be considered as possible track candidate extensions. Thus, the area of interest can be defined by two angles *epsphilower* and *epsphihigher* shifted from the track candidate's last accepted hit azimuthal angle ϕ in the direction defined by the particle charge (Fig. 2b).

2.2. Secondary Tracks

Secondary tracks can be produced in decays of particles or their interactions with a detector material and
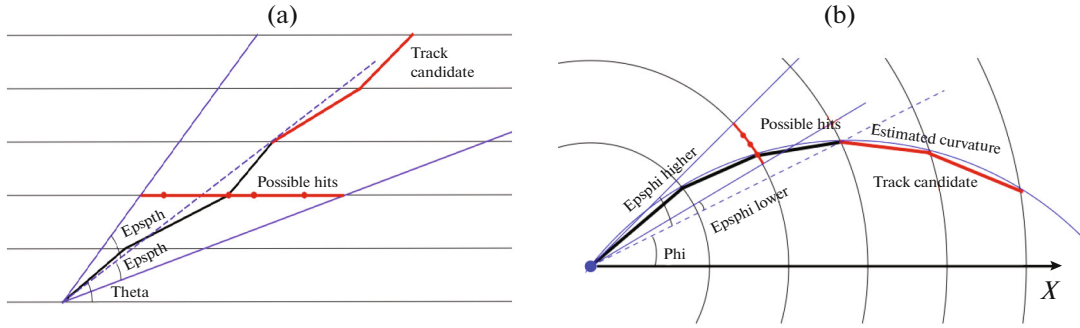
Fig. 2. (a) Track scheme in longitudinal projection. (b) Track scheme in transverse projection.

the position of their origin is not a priori known. Therefore, it can not be used in the track model and track propagation should rely on the information from the earlier propagation steps. For the track finding method under consideration the track evolution scheme is quite simple. Namely, in the longitudinal projection it is possible to use a linear track extrapolation from the accepted hit to the following layer according to the formula:

$$z_{\text{next}} = z_{\text{curr}} + \frac{z_{\text{prev}} - z_{\text{curr}}}{r_{\text{prev}} - r_{\text{curr}}} (r_{\text{next}} - r_{\text{curr}}), \qquad (1)$$

where $z_{\text{curr}}, z_{\text{prev}} (r_{\text{curr}}, r_{\text{prev}})$ are the z-positions and radii of the hits on the current and previous layers, respectively, and z_{next} is the extrapolated z-position at the next layer with radius r_{next}. In the transverse projection, a circle arc track model can be used to do the extrapolation to the next detector layer. To be defined, both propagators require some minimum number of points, i.e. two for the longitudinal projection and three for the transverse one. While the first point does not have any constraints, the others can be selected still using the primary vertex position since it only defines the general track direction and not the acceptance window size as discussed in the next section.

3. DETERMINATION OF CONSTRAINTS

Since the described method is based on a priori constraints, the important part of the toolkit deals with the task of obtaining them. In practice, it contains ROOT macros to extract necessary distributions from Monte Carlo simulated events and define hit acceptance windows. The studied data of central Au + Au collisions at center-of-mass energy $\sqrt{s_{NN}} = 9$ GeV were produced with the UrQMD event generator [6] and transported through the detector set-up using GEANT3 particle transport code to simulate ITS hits within the MpdRoot software framework [7]. It should be noted here, that reconstruction of secondary particles is not a well defined task since they can be produced virtually everywhere inside the detector. For

the current study, only the ones created inside the innermost barrel, i.e. closer to the beam line than the innermost layer, were considered. This is quite justified since the ITS primary purpose is to reconstruct secondary particles produced very close to the primary vertex from decays of short-lived objects.

In Fig. 3 the polar and azimuthal angle differences of hits on consecutive layers from primary particles are shown as functions of particle transverse momentum. One can see that the transverse window definition requires knowledge of the transverse momentum, which can be estimated with sufficient accuracy from positions of 2 hits and the primary vertex (Fig. 4a). Corrected for the track curvature with the function $\sim 1/p_T$, the azimuthal angle difference is shown in Fig. 4b. Together with Fig. 3a they should be used to select window sizes in two directions. To preserve the selection efficiency and, at the same time, not to compromise on the processing speed, the algorithm is implemented as a two-step procedure. At the first pass, relatively narrow window is taken to find high-p_T tracks. After track verification with the Kalman fitter the assigned hits are tagged as used ones and not considered during other passes. During the second pass window sizes are increased to find lower-p_T tracks.

For secondary particles, utilization of the same selection variables (θ and ϕ) is not optimal, as can be seen in Fig. 5 where polar and azimuthal angle differences between hits on consecutive layers are shown. One can see that although the overall patterns are similar to those for primary tracks, there is also a significant spread of points. As can be seen in Fig. 6, using linear extrapolation of the longitudinal coordinate z according to Exp. (1) and circle arc propagator in transverse projection give much better point localization. However, these methods require at least two and three hits for longitudinal and transverse projections, respectively. Therefore, to perform the linear extrapolation to the layer 4 and circular one to the layer 3, the procedure still relies on the approximation that the track comes the primary vertex. As can be seen in Fig. 7, this assumption gives quite reasonable results,
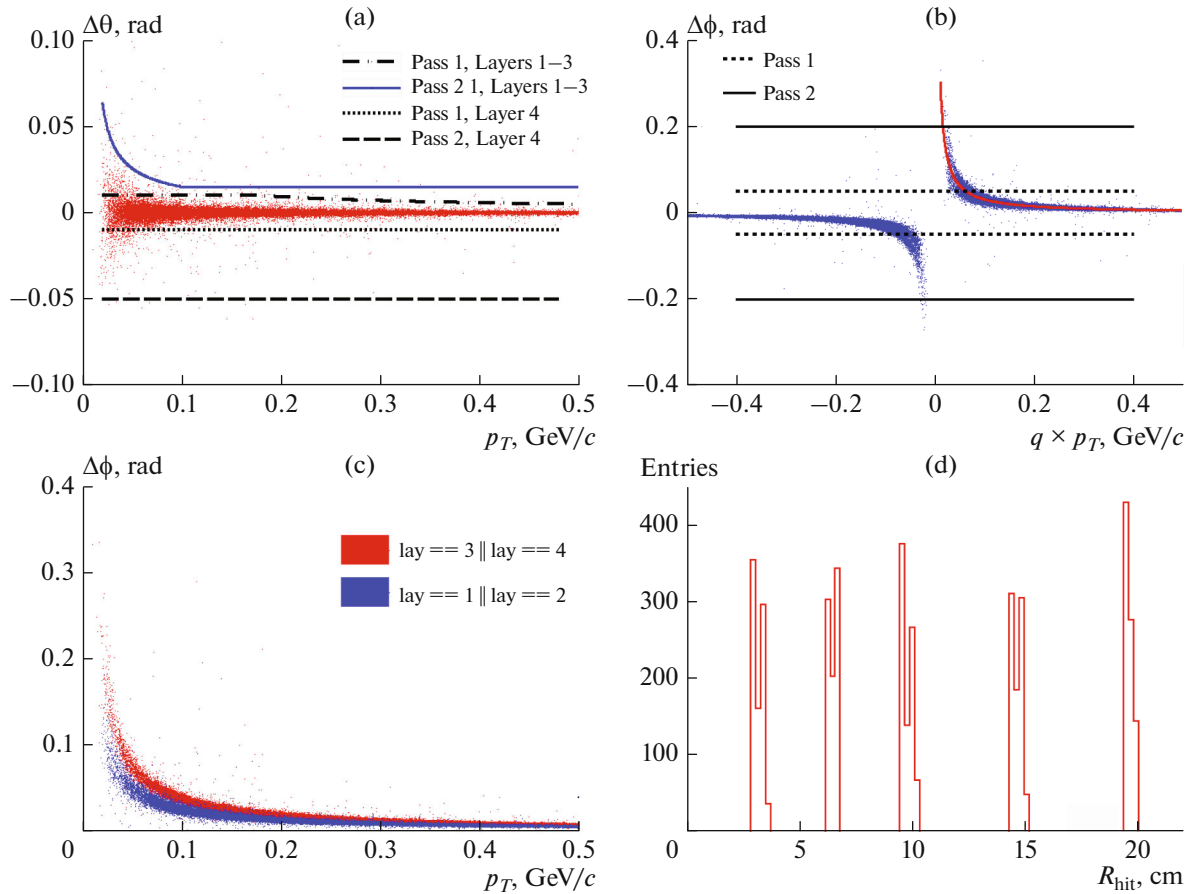
Fig. 3. (a) Polar angle difference of hits on consecutive layers from the same primary particle as a function of transverse momentum. Lines show hit acceptance windows: dotted and dashed lines are for reconstruction passes 1 and 2 on ITS layer 4 (only negative values are drawn), dash–dotted and solid lines are for passes 1 and 2 on layers 1–3 (only positive values are drawn). (b) Azimuthal angle difference of hits on consecutive layers from the same primary particle as a function of the signed transverse momentum (where the sign corresponds to the particle charge). Red curve shows result of the fit to the function $\sim 1/p_T$. Dashed and solid horizontal lines show acceptance windows for pass 1 and 2 on layer 4. (c) The same as in Fig. 3b for positive particles: blue dots for two innermost layers, red ones for next two layers (difference comes from the difference in radial distance between layers—in Fig. 3d. d) Distribution of ITS hits radii.
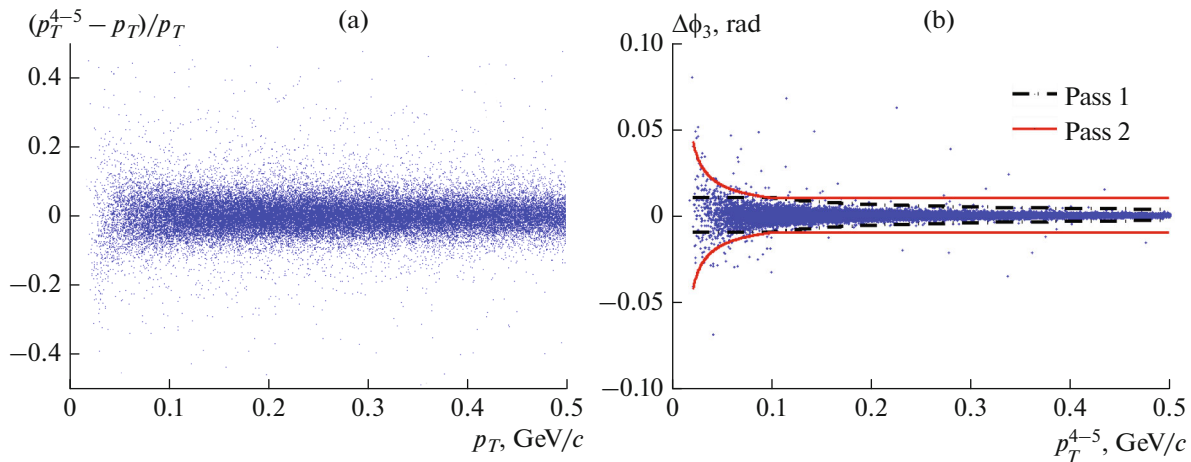

Fig. 4. (a) Relative transverse momentum resolution for primary tracks, where the momentum is reconstructed using hits from the two outermost layers 4 and 5 and the primary vertex. (b) Azimuthal angle reconstruction uncertainty on layer 3 $\Delta\phi_3$ from a hit on layer 4 and estimated track momentum p_T^{4-5}. Dash–dotted and solid lines show acceptance windows for passes 1 and 2 on ITS layers 1–3.
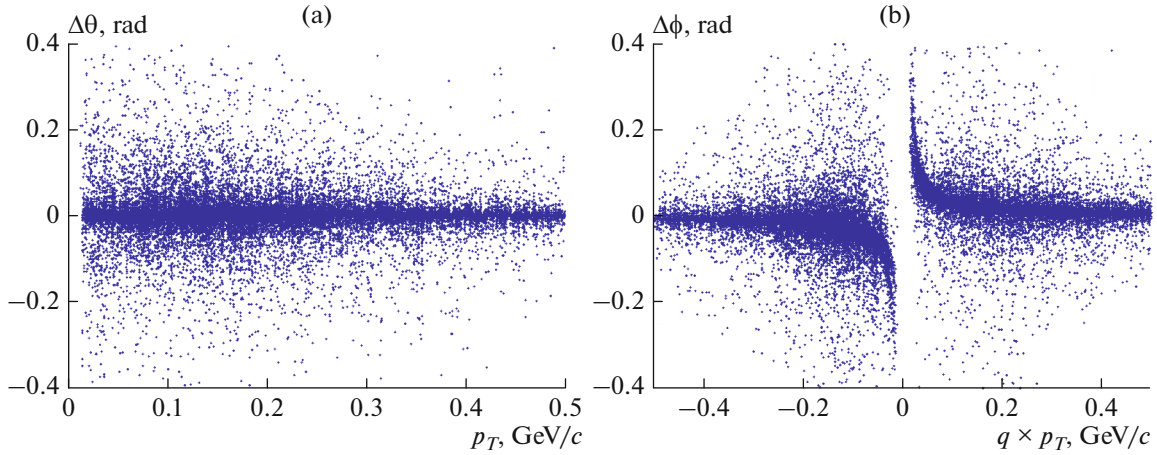
Fig. 5. (a) Polar angle difference of hits on consecutive layers from the same secondary particle as a function of transverse momentum. (b) Azimuthal angle difference of hits on consecutive layers from the same secondary particle as a function of signed transverse momentum.
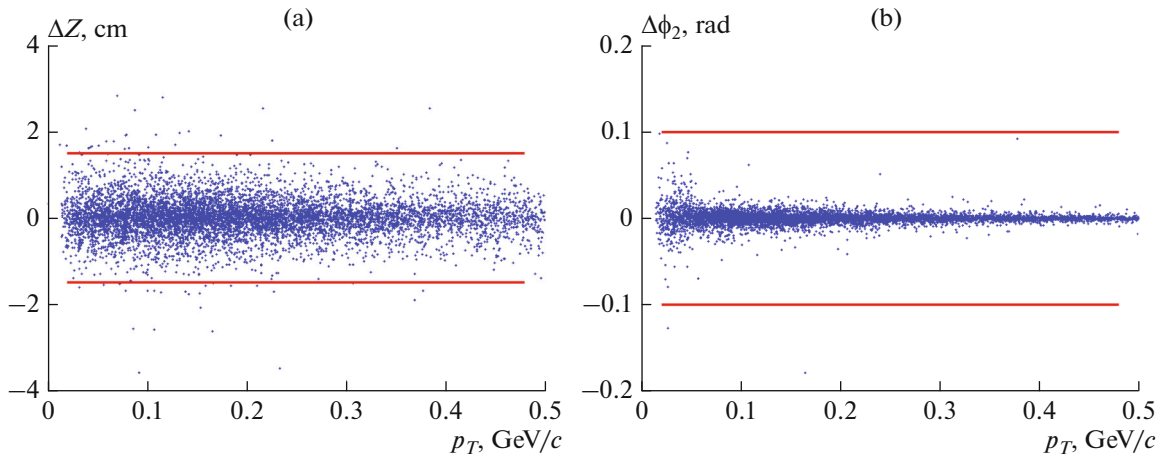

Fig. 6. (a) Longitudinal coordinate z uncertainty of hits on layer 3 estimated from hits on layers 4 and 5 using Expr. (1) as a function of p_T for secondary tracks. (b) Azimuthal angle extrapolation error on layer 2 for secondary particles using circle arc model versus p_T. Lines show hit acceptance windows.

at least for tracks produced inside the innermost detector barrel. Moreover, for this reconstruction pass the number of hits is already significantly reduced and one can afford to use relatively wide windows without increasing the processing time.

4. PERFORMANCE RESULTS

Performance of the approach presented was evaluated on the same data which were used to define hit acceptance windows for the tracking, i.e. simulated central Au + Au events at $\sqrt{s_{NN}} = 9$ GeV. Track reconstruction efficiencies shown below are calculated for particles having hits in at least 3 ITS layers and include so-called "good" reconstructed tracks, i.e. containing more than 50% of hits from the same particle. Particle

multiplicities of the processed events are shown in Fig. 8. One can see that the mean multiplicity is close to 1000, secondary particles comprise about 13%, and ~64% of them are produced inside the innermost barrel.

As can be seen in Fig. 9, the method demonstrates high efficiency both for primary and secondary tracks, i.e. close to 100% in central region ($|\eta| < 1.2$) down to $p_T \simeq 0.05$ GeV/c and for $p_T > 0.1$ GeV/c up to $|\eta| \simeq 1.8$. At the same time, the contamination rate, defined as percentage of clone and ghost tracks, is quite low (Fig. 10). Here clones are multiple "good" tracks found for one particle and ghosts are bad (not "good") tracks. The track reconstruction quality can also be estimated from Fig. 11, where the relative transverse momentum resolution and track pointing accuracy are
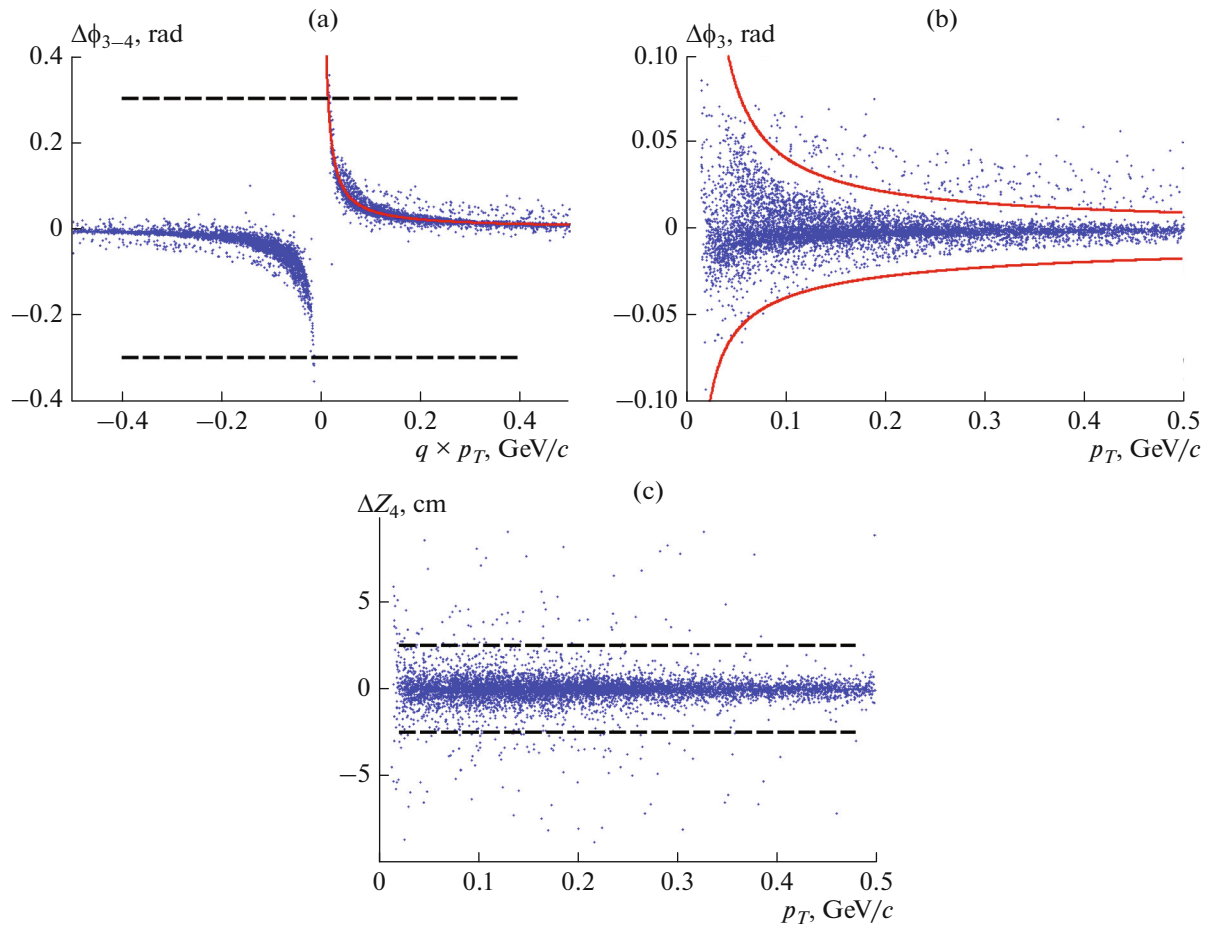
Fig. 7. (a) Azimuthal angle difference between layers 4 and 3 $\Delta\phi_{3-4}$ for secondary particles as a function of reconstructed p_T. Line shows result of the fit to the function $\sim 1/p_T$. (b) Azimuthal angle extrapolation error on layer 3 $\Delta\phi_3$ for secondary particles using the fitted function versus p_T. (c) Longitudinal coordinate z uncertainty of hits on layer 4 Δz_4 estimated using hits on layer 5 and the primary vertex. Lines show hit acceptance windows.
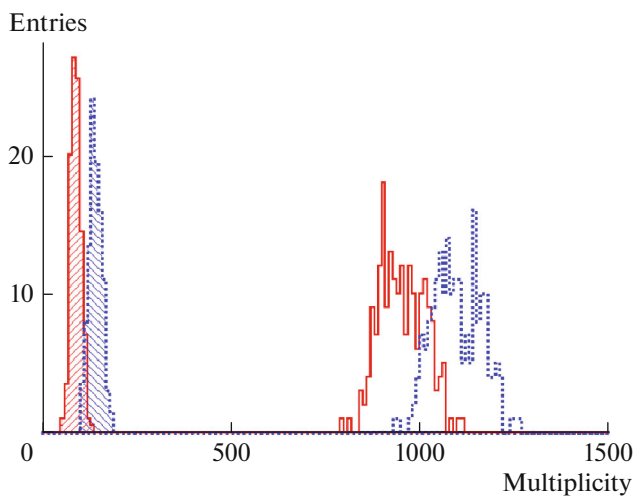

Fig. 8. Particle multiplicity seen in the ITS: at least one layer is hit (empty dashed histogram), at least 3 layers (empty solid), secondaries with at least 3 layers (dashed hatched), ~64% of which are produced within 2.9 cm from the beam line (solid hatched).

shown as functions of p_T for primary tracks in central region ($|\eta| < 1.2$). Here the track pointing accuracy is defined as transverse and longitudinal position errors at the point of the closest approach (PCA) to the interaction point.

It is also quite informative to compare, for example, the efficiency for the presented method and the one based on the TPC track propagation through the ITS (although the latter by construction includes the TPC-ITS matching part with its inefficiency and extra processing time). Figure 12 shows that Vector Finder demonstrates a visible efficiency improvement for "good" tracks from the same event sample and this performance gain is achieved with a factor of ~2 lower time consumption (2.2 versus 4.7 s/event).

5. SUMMARY AND NEXT STEPS

A track reconstruction approach based on a combinatorial hit search has been developed and implemented as a Vector Finder toolkit. The method has
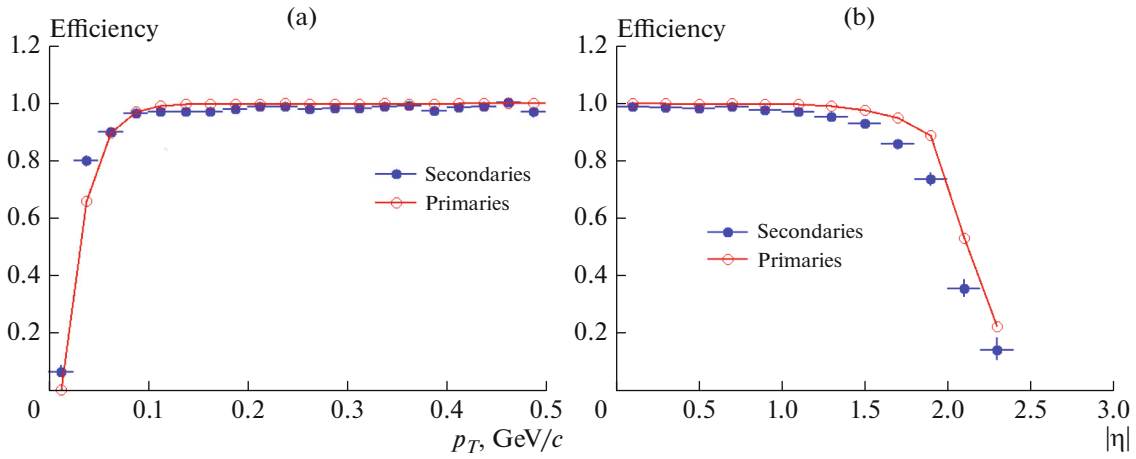
Fig. 9. (a) Reconstruction efficiency as a function of transverse momentum for primary and secondary tracks produced with $|\eta| < 1.2$; (b) Reconstruction efficiency as a function of $|\eta|$ for primary and secondary tracks with $p_T > 0.1$ GeV/c. Red color is for primaries, blue one for secondaries.
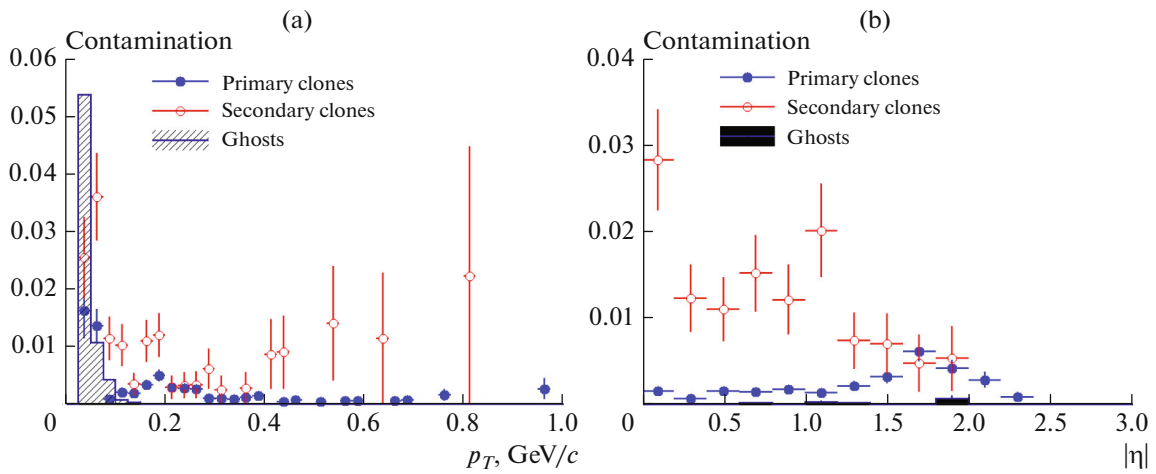

Fig. 10. (a) Percentages of clones and ghosts versus p_T. (b) Percentages of clones and ghosts versus $|\eta|$.
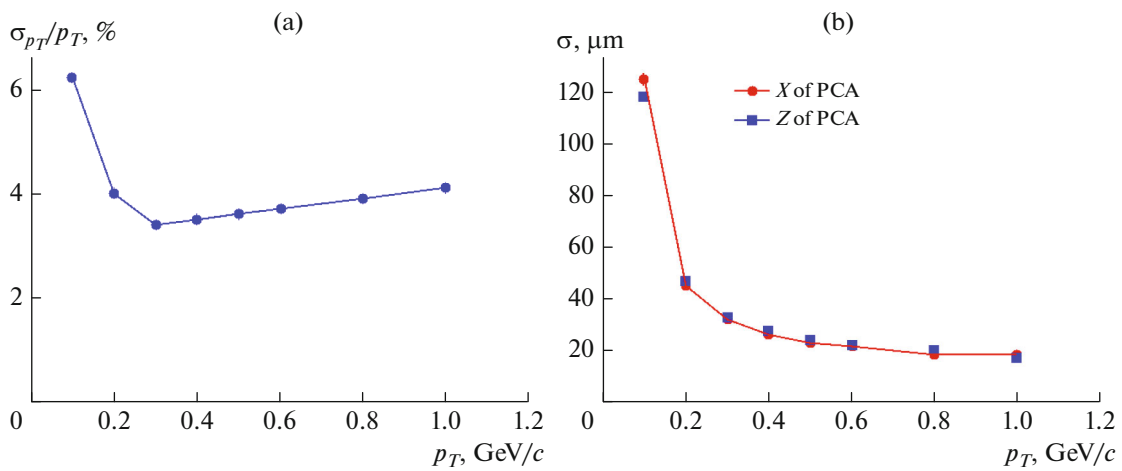

Fig. 11. (a) Relative transverse momentum resolution as a function of p_T for primary tracks. (b) Track pointing accuracy versus p_T for primary tracks.
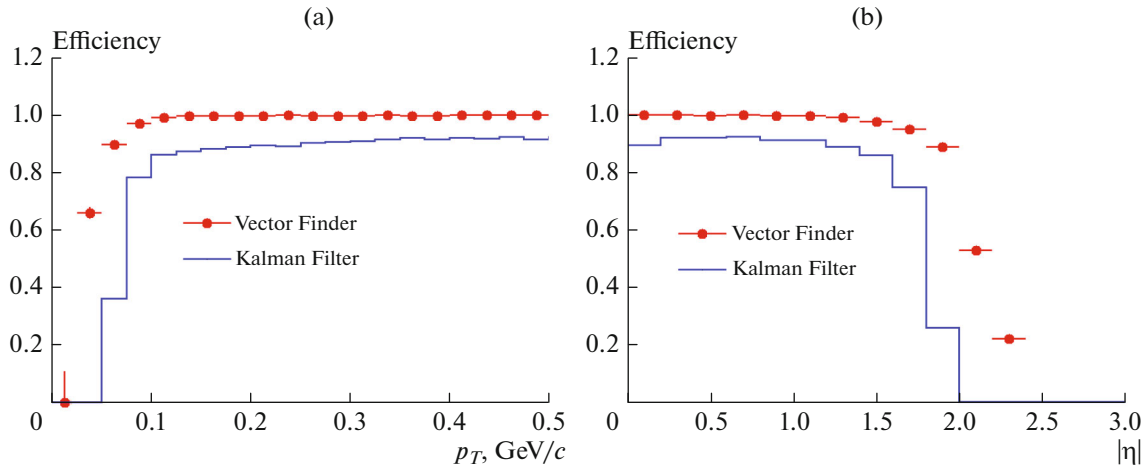
Fig. 12. (a) Reconstruction efficiency as a function of transverse momentum for primary particles at $|\eta| < 1.2$ obtained with the Vector Finder and TPC-based Kalman Filter methods. (b) Reconstruction efficiency versus $|\eta|$ for $p_T > 0.1$ GeV/c.

been described and the hit acceptance strategy explained. Good performance results have been demonstrated on Monte Carlo simulated high multiplicity event samples.

As the next steps, it is planned to implement the ITS-TPC matching procedure and apply the combined package for performance studies and design optimization of the MPD ITS.

6. ACKNOWLEDGMENTS

FUNDING

REFERENCES

1. V. D. Kekelidze, R. Lednicky, V. A. Matveev, I. N. Meshkov, A. S. Sorin, and G. V. Trubnikov, "Three stages of the NICA accelerator complex," Eur. Phys. J. A **52**, 211 (2016).
2. V. Golovatyuk, V. Kekelidze, V. Kolesnikov, O. Rogachevsky, and A. Sorin, "The multi-purpose detector (MPD) of the collider experiment," Eur. Phys. J. A **52**, 212 (2016).
3. B. Abelev et al. (ALICE Collab.), "Technical design report for the upgrade of the ALICE inner tracking system," J. Phys. G **41**, 087002 (2014).
4. D. Zinchenko, E. Nikonov, and A. Zinchenko, "A track finding algorithm for the inner tracking system of MPD/NICA," EPJ Web Conf. **204**, 07006 (2019).
5. D. Zinchenko, A. Zinchenko and E. Nikonov, "A 'vector finder' approach to track reconstruction in the inner tracking system of MPD/NICA," AIP Conf. Proc. **2163**, 060006 (2019).
6. http://urqmd.org/.
7. K. Gertsenberger, S. Merts, O. Rogachevsky, and A. Zinchenko, "Simulation and analysis software for the NICA experiments," Eur. Phys. J. A **52**, 214 (2016).